Adsorption Characteristics of Benzene on Electrospun-Derived Porous Carbon Nanofibers

Wang Geun Shim,[1] Chan Kim,[1,3] Jae Wook Lee,[2] Je Jung Yun,[1] Young Il Jeong,[1] Hee Moon,[1,3] Kap Seung Yang[1,3]

[1]*Faculty of Applied Chemical Engineering, Chonnam National University, Gwangju 500-757, Korea*
[2]*Department of Environmental and Chemical Engineering, Seonam University, Namwon 590-170, Korea*
[3]*Center for Functional Nano Fine Chemicals (BK21 CFN), Chonnam National University, Gwangju 500-757, Korea*

Received 30 November 2005; accepted 24 March 2006
DOI 10.1002/app.24554
Published online in Wiley InterScience (www.interscience.wiley.com).

ABSTRACT: The adsorption properties of polyacrylonitrile (PAN) carbon nanofibers fabricated by using an electrospinning route were assessed for their applicability as a novel alternative adsorbent. Commercial fiber, A–10, was chosen for comparison. Nitrogen adsorption/desorption isotherms and gravimetric techniques were used to examine the porous structure, adsorption equilibrium, kinetics, and the energetic heterogeneity of the prepared adsorbent. The nitrogen adsorption and desorption isotherms showed that PAN carbon nanofibers are highly microporous with small amounts of mesoporous regions. The equilibrium data of benzene was obtained at three different temperatures (343.15, 383.15, and 423.15) K with pressures up to 4 kPa. The data correlated successfully with the Toth isotherm equation. In addition, by using this isotherm model, the adsorption affinity and isosteric enthalpy of adsorption were determined. The results of the isosteric enthalpy of adsorption and adsorption energy distribution tests/equations revealed that although PAN carbon nanofibers have a heterogeneous surface, they seem to be more homogeneous than commercial carbon fibers. Moreover, the mass transfer and thermal desorption results showed that shallow pores contained within PAN carbon nanofibers may be effective adsorbents for removing toxic compounds. © 2006 Wiley Periodicals, Inc. J Appl Polym Sci 102: 2454–2462, 2006

Key words: simulations; adsorption; kinetics (polym.); fibers; modeling

INTRODUCTION

The proper recovery and control of volatile organic compounds (VOCs) from industrial facilities is very important in reducing production cost, saving energy, and protecting the environment. Over the past few decades, much attention has been focused on finding cost-effective pollution-prevention techniques. However, many of the well-known VOC control mechanisms have several advantages and limitations. For example, the adsorption process has been widely useful for treating VOCs because of its higher selectivity and relatively higher capacity for organic molecules even at low partial pressures. In general, the adsorbents used in adsorption-based methods are considered essential in performing the best removal efficiency of VOCs. Yet, the performance of these adsorbents is highly dependent on the adsorption amount, kinetics, and regeneration (or desorption). Until now, activated carbon has been known as the most proper adsorbent for this purpose, since it has several advantages, namely: (1) easy operation, (2) low operating cost, and (3) efficient recovery of most VOCs. On the other hand, a considerable number of studies have been conducted on the development of alternative adsorbents such as activated carbon fibers (ACFs), hydrophobic zeolite, polymer resins, and mesoporous media for overcoming the severe problems associated with activated carbons such as combustion at high temperature, pore blocking, and hygroscopic property.[1,2] Among them, ACFs are considered the most promising alternative material because of their chemical and thermal stability, high adsorption capacities, rapid adsorption rates, and hydrophobic tendencies. Previous studies have shown that ACFs exhibit a larger adsorption and desorption amount (or working capacity) than other adsorbents.[3,4]

Among the various technologies available for the fabrication of fibers, the electrospinning method has been widely used for the application of ultrafiltration, composite reinforcements, tissue engineering, drug deliver carrier, catalysis, and nanoelectronics, since it provides a fast, simple, and cost-effective route to produce ultrafine fibers with diameters ranging from 1 nm to 1 μm.[5–9] Recently, Kim and Yang [5] have reported that polyacrylonitrile (PAN) carbon nanofibers, which are produced by using a nonwoven web, have high specific surface areas with a shallow pore size formed through carbonization and activation processes. Even though studies on organic adsorption are very limited,

Correspondence to: H. Moon (hmoon@chonnam.ac.kr) or K. S. Yang (ksyang@chonnam.ac.kr).

Contract grant sponsor: Korea Science and Engineering Foundation; contract grant number: R01-2005-000-10,742-0.

some results have indicated that PAN carbon nanofibers can be efficiently applied as electrodes for super capacitors.[7]

The primary goal of this study is to investigate the adsorption equilibrium, thermal desorption, and kinetics of organic compound and assess its possibility as an alternative adsorbent with commercial ACFs, A–10. The PAN carbon nanofibers were fabricated and characterized by using the electrospinning and nitrogen adsorption–desorption methods. A–10, well-known adsorbents for various reasons, were chosen to be a standard adsorbent to compare with PAN carbon nanofibers. Benzene was also used as a reference compound for the assessment of properties of both adsorbents. Adsorption amount, adsorption, and thermal desorption curves of benzene were measured accurately by using a gravimetric apparatus. To explain the adsorption equilibrium data and to determine the isosteric enthalpy of adsorption and affinity constant of adsorbate, the thermodynamically consistent Toth equation was used. In addition, adsorption energy distribution was evaluated using a generalized nonlinear regularization method to understand the energetic heterogeneity of PAN carbon nanofibers. The homogeneous surface diffusion model (HSDM) was also used to determine the adsorption rates.

EXPERIMENTAL

Sample preparation and characterization

Electrospun porous carbon nanofibers were prepared using the procedures describe in our previous work.[5] PAN ($M_w = 180{,}000$ homopolymer) was dissolved at concentration of 10 wt % in *N*,*N*-dimethylformamide (DMF). The solution was spun into the fiber web through a positively charged capillary, using an electrospinning apparatus at 20 kV dc and the tip to collect distance (TCD) between the tip of syringe and the collector was 18 cm (NT-PS-35K, NTSEE, Korea). The electrospun fiber web was stabilized by heating it at 1°C/min up to 280°C and by holding it for 1 h under an air current. The stabilized fiber webs were heated at a rate of 5°C/min for up to 800°C in a flow of nitrogen, and then the webs were activated by using a volume of 30% steam in a carrier gas of nitrogen for 60 min. The commercial activated carbon fibers, A–10 (ACFs) were supplied by At'all (Osaka gas and Unitika, Japan). The microtextural characterization of the samples was performed by scanning electron microscopy (SEM, Hitachi, *S*-4700, Japan), and by nitrogen adsorption–desorption at 77 K (Micromeritics, ASAP 2020, USA).

Gravimetric apparatus

The adsorbed amount of solvent vapors was measured by using a quartz spring balance placed in a closed glass system. The benzene vapor was generated in a small chamber that was maintained at a constant temperature. A given amount (0.1 g) of adsorbents was placed on the dish attached to the end of the quartz spring. Adsorbent samples were weighed with an accuracy of $\pm$ 0.01 mg. This system was vacuumed for 12 h at 10^{-3} Pa and 523.15 K to remove volatile impurities from the fibers. A turbomolecular pump (Edward type EXT70) in combination with a rotary vacuum pump (Edward model RV5) was used to evacuate the system. Pirani and Penning vacuum gauges (Edwards Series 1000) were used for the measurement of vacuum. The pressure of the system was measured using a Baratron absolute pressure transducer (MKS instruments type 128), with the accuracy of $\pm$ 0.15%, and a power supply read out instrument (Type PDR-C-1C). The variation of mass was measured by a digital voltmeter that is connected to the spring sensor. Equilibrium experiments were carried out at three temperatures of (343.15, 383.15, and 423.15) K, respectively.[10,11]

RESULTS AND DISCUSSION

Adsorption isotherms

Figure 1 shows the FE-SEM images of PAN carbon nanofibers and commercial ACFs of A–10. The PAN carbon nanofibers exhibit long and straight fibrous morphology with homogeneous diameters ranging from 200 to 300 nm. The average diameters of the PAN carbon nanofibers and A–10 are 250 nm and 20 μm, respectively. The diameters of PAN carbon nanofibers are about 100 times smaller than the A–10. These small diameters are directly related to the benzene adsorption kinetics, which will be discussed in the following paragraphs.

In general, the nitrogen adsorption and desorption method has become an useful and reliable standard technique for obtaining the valuable information on the surface characteristics of porous adsorbents such as surface area, pore size, and pore volume, because of relatively small molecular size of the gas. Figure 2 presents the nitrogen adsorption and desorption isotherms of two samples (PAN carbon nanofibers and A–10) at 77 K. As shown in this figure, all isotherms are reversible and do not exhibit significant hysterisis loops between adsorption and desorption branches. The adsorption amount of nitrogen for PAN carbon nanofibers sample synthesized by the electrospining method (or proposed method) was much larger than a sample of commercial A–10. Moreover, the isotherms of nitrogen obtained here can be identified as Type I on the basis of IUPAC classification that represents the long plateau indicating the adsorption characteristics of microporous adsorbents. The figure also shows that the adsorbed amount of nitrogen on these samples

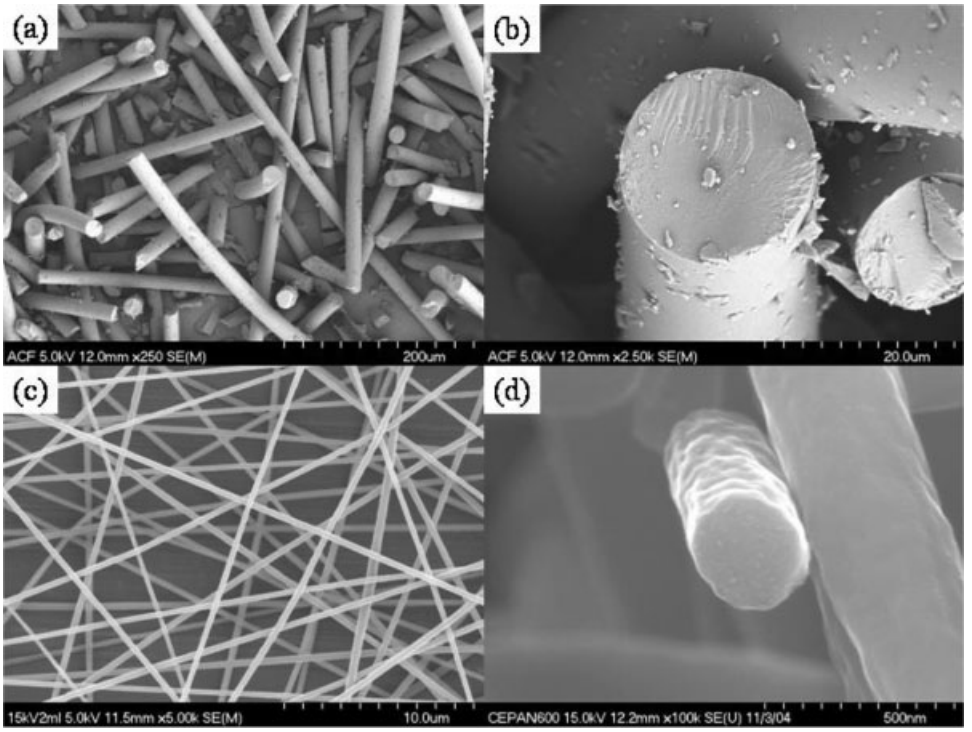

Figure 1 Low magnification and cross-sectional FE-SEM images of activated carbon fibers; (a), (b) A–10, and (c), (d) PAN carbon nanofibers

increases rapidly up to the relative pressure of about 0.2, and then approaches a marginally sloping plateau. The graph then extends to a range from about 0.2 to 1.0 for existing micropores and small mesopores. These results are similar to those of a previous report.[12] Li et al.[12] suggested that the adsorption properties of these materials could be explained by: (i) the primary filling in very narrow micropores, (ii) the formation of a monolayer in wider micropores and small mesopores, and (iii) the filling of the larger micropores and mesopores by capillary condensation process.

Table I summarizes the important pore structure parameters such as BET-specific surface area, total pore volume, micropore volume, and average pore diameter of A–10 and PAN carbon nanofibers. On the whole, the PAN carbon nanofibers provide a slightly higher surface area and pore volume than that of commercial fiber A–10. However, the average pore diameters of these samples give similar values.

Adsorption equilibrium isotherm data with a wide range of temperature and concentrations provide essential information in understanding, analyzing, designing, and optimizing the adsorption separation processes. Therefore, in this work, benzene was used as a model compound for comparative analysis of two selected activated carbon fibers. The adsorption

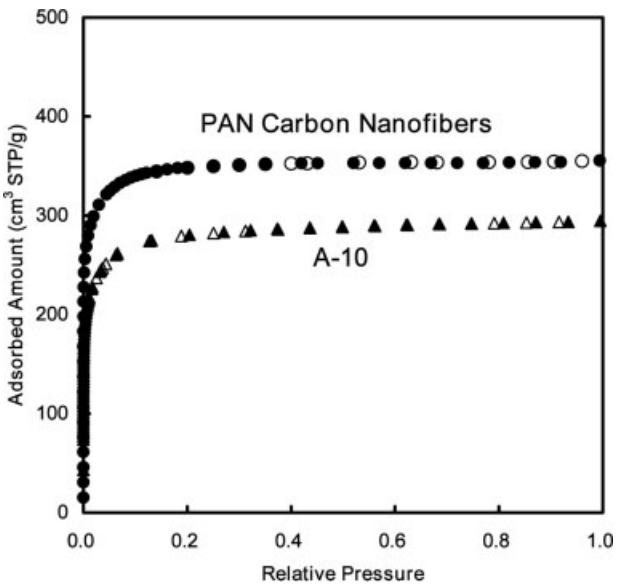

Figure 2 Nitrogen adsorption–desorption isotherms at 77 K.

TABLE I
Physical Properties of PAN Carbon Nanofibers and A–10

Property	PAN carbon nanofibers	A–10
Specific surface area[a] ($m^2\ g^{-1}$)	1193	1015
Average pore size[b] (Å)	23	22
Micropore volume[c] ($cm^3\ g^{-1}$)	0.455	0.432

[a] Specific surface area calculated by BET method.
[b] Average pore size calculated with BJH method.
[c] Micropore volume calculated with HK method.

equilibrium isotherm data was obtained at temperatures in the range of 343.15–423.15 K with pressure up to around 4 kPa for A–10 and PAN carbon nanofibers. Figure 3 shows the adsorption equilibrium data of benzene on activated carbon fibers that were also found to be Type I according to the IUPAC classification that exhibits stronger attractive forces between the adsorbate and adsorbent. The experimental results revealed that the novel fiber (PAN carbon nanofibers), which exhibited slightly large specific surface area, had a higher adsorption capacity than that of A–10 at the same condition.

Adsorption isotherm equations are also crucial for model prediction in adsorption-based technologies. To apply the practical application system, the obtained experimental equilibrium data must correlate with the analytical form. Many equilibrium models have been developed, proposed, and used to explain various adsorption systems over the years. Among them, the Toth equation has been popularly used for heterogeneous adsorbents such as microporous-activated carbon and activated carbon fiber, because of its simplicity and accuracy at both low and high pressures.[13,14] The Toth equation is as follows:

$$N = \frac{mP}{(b + P^t)^{1/t}} \tag{1}$$

where P is equilibrium pressure, N is adsorbed moles, and m, b, and t are isotherm parameters. The Toth equation is reduced to the well-known Langmuir equation when the parameter t approaches 1. Therefore, the parameter t is said to characterize the system heterogeneity. Also, the thermodynamic consistency test of the isotherm equation used is important. Although the Toth equation is an empirical equation, it approaches the Henry constant at low pressures and the saturation limit at high pressures.

$$H = \lim_{P\to 0} \frac{N}{P} = \lim_{P\to 0} \frac{dN}{dP} = \frac{m}{b^{1/t}} \tag{2}$$

$$\lim_{P\to \infty} N = m \tag{3}$$

The adsorption isotherm parameters were determined from experimental equilibrium data using a pattern search algorithm called Nelder–Mead simplex method.[15] The used objective function is based on the square of residuals (SOR), which is an absolute value and the magnitude of the determined value is also closely related with its accuracy and the number of experimental points. The SOR was expressed as follows:

$$\mathrm{SOR} = \frac{1}{2}\sum (N_{\mathrm{exp}} - N_{\mathrm{cal}})^2 \tag{4}$$

where N_{cal} and N_{exp} are the calculated and experimental amounts adsorbed, respectively. All the isotherm parameters and SOR values determined are summarized in Table II. As shown in Figure 3, the solid lines are the predicted results of benzene on two carbon fibers, by the Toth equation. The isotherm model represents the experimental data fairly well for the pressure and temperature range studied. In addition, the extracted system heterogeneity parameters for A–10 and PAN carbon nanofibers are in the ranges of 0.30–0.36. This result implies that the selected and manufactured carbon fibers are energetically heterogeneous since the values of t significantly deviate from unity.

In general, the Henry constant reveals the properties of adsorbent and adsorbate. Thus, as a criterion of

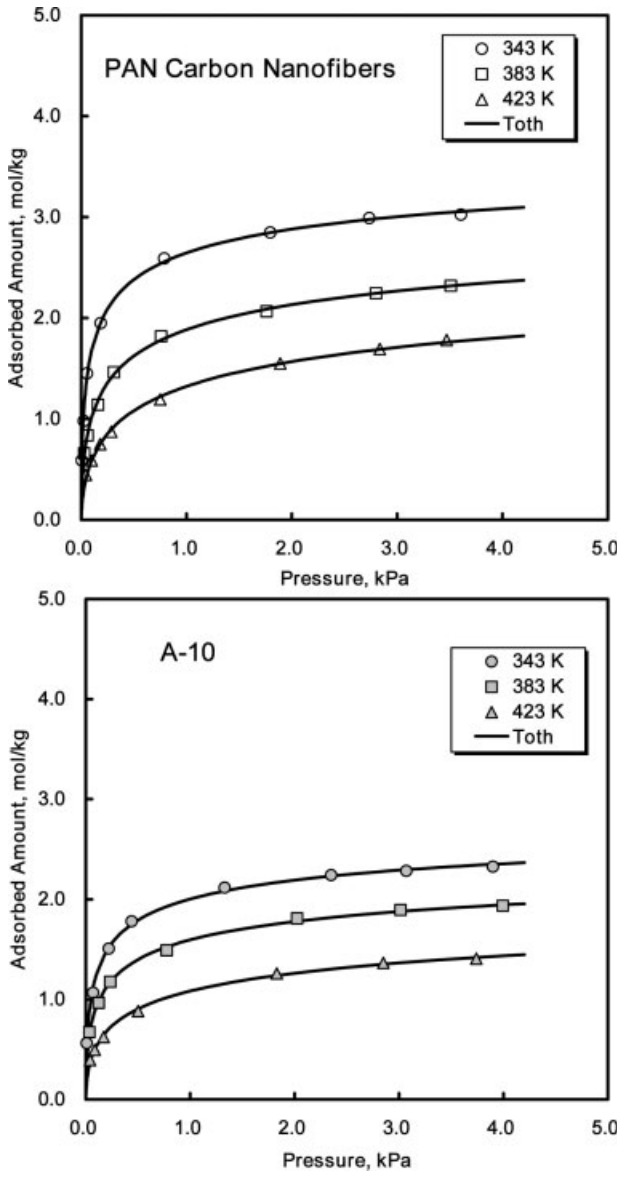

Figure 3 Adsorption equilibrium isotherms of benzene on PAN carbon nanofibers and A–10.

TABLE II
Toth Equation Parameters for Benzene Vapor

Adsorbent	Temp (K)	m (mol kg^{-1})	b (kPa)	t	SOR
PAN carbon nanofibers	343.15	3.965	0.159	0.364	0.0086
	383.15	3.585	0.244	0.339	0.0026
	423.15	3.344	0.366	0.336	0.0018
A–10	343.15	3.081	0.169	0.363	0.0035
	383.15	2.825	0.209	0.331	0.0018
	423.15	2.656	0.313	0.304	0.0014

adsorption affinity, it is useful for understanding the adsorption system. By using the Toth isotherm equation, Henry's law constants were calculated and plotted in Figure 4 (top). Although the calculated Henry's law constants are extrapolations based on the isotherm used, this procedure has been accepted when discussing adsorption affinity. The determined Henry constants of PAN carbon nanofibers studied at 343.15, 383.15, and 423.15 K were 625, 232, and 67 mol kg^{-1} kPa^{-1}, respectively. On the other hand, in the case of A–10, the affinity values derived for the same temperature ranges were 414, 320, and 121 mol kg^{-1} kPa^{-1}, respectively. As shown in this figure, PAN carbon nanofibers had higher affinity than A–10 at lower adsorption temperatures (<343.15 K). However, the order of adsorption affinity reversed when the temperature was above 383.15 K. The isosteric enthalpy of adsorption at zero loading, q_0^{st}, can also be obtained from the Henry constant as follows[11]:

$$\frac{q_0^{st}}{RT^2} = -\left[\frac{\partial \ln H}{\partial T}\right] \tag{5}$$

where, R is the gas constant, T is the temperature, and H is Henry's constant. The plot on both samples shows linearity for benzene molecules. Hence, the value of q_0^{st} can be obtained from the slope. The determined q_0^{st} values of benzene are about 33 kJ mol^{-1} for A–10 and 18 kJ mol^{-1} for PAN carbon nanofibers.

The isosteric enthalpy of adsorption represents the interaction properties of the adsorbent–adsorbate molecules or the adsorbate–adsorbate in the adsorbed phase, and it has been widely used in characterizing the adsorption system. If the adsorption system follows the ideal case (Langmuir isotherm), which means adsorption energy is constant over all sites, the isosteric enthalpy of adsorption is independent of the adsorbed amount. However, in the case of an energetically heterogeneous surface, the curve for isosteric enthalpy of adsorption varies with the surface loading. In other words, the adsorbate–solid surface interaction (or vertical interaction) energy decreases with increasing moles adsorbed and the adsorbate–adsorbate lateral interactions increase as the coverage increases. Therefore, information concerning the magnitude of the enthalpy of adsorption and its variation with coverage can provide useful information about the nature of the surface and the adsorbate phase. The isosteric enthalpy of adsorption (q_{st}) can be calculated by using the Clausius–Clapeyron equation, if an excellent set of

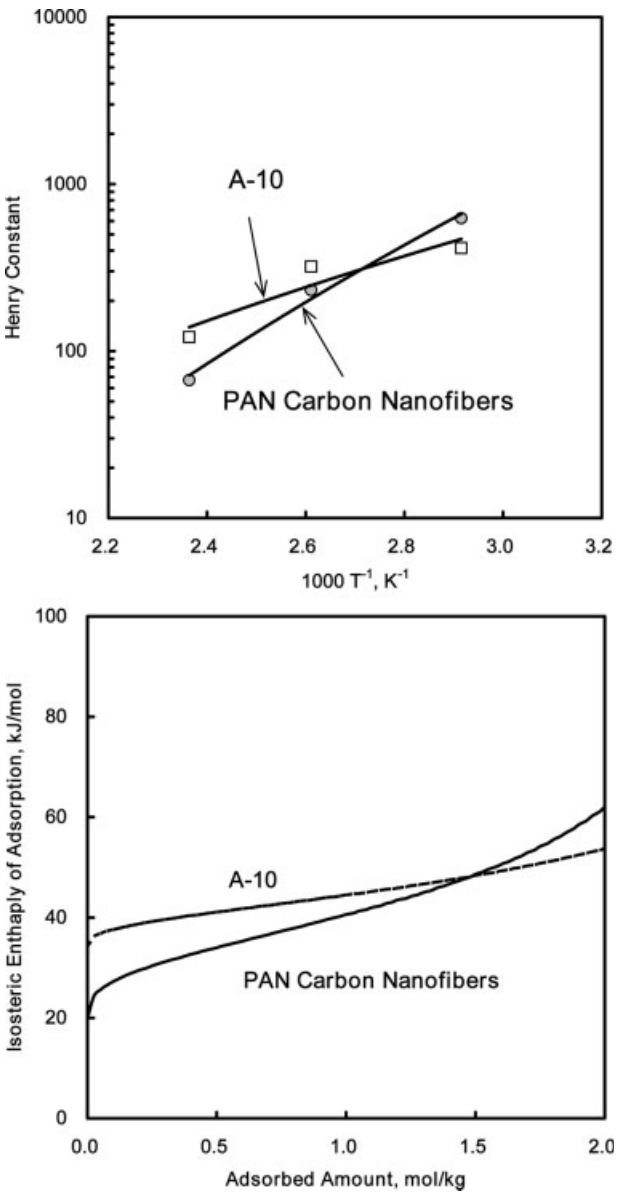

Figure 4 Henry's constant of adsorption for various temperatures (top) and Isosteric enthalpy of adsorption of benzene (bottom).

adsorption equilibrium data is obtained at several temperatures.[16]

$$\frac{q_{st}}{RT^2} = \left[\frac{\partial \ln P}{\partial T}\right]_N \quad (6)$$

In Figure 4 (bottom), the isosteric enthalpy of adsorption for two adsorbents calculated using Toth isotherm model is plotted as a function of the moles adsorbed. As shown in this figure, the isosteric enthalpy curves continuously increases as the surface loading increases for benzene vapor on each adsorbent. In addition, the change of isosteric enthalpy of adsorption for A–10 investigated is more distinctive than that of PAN carbon nanofibers, with an increase in moles adsorbed. Also, PAN carbon nanofibers have higher values of q_{st} than A–10 in the amount of moles adsorbed, ranging from zero up to about 1.5 mol kg^{-1}. This result implies that the fibers studied here have energetically heterogeneous surfaces.

Adsorption energy distribution

In general, the surfaces of porous adsorbents have complex geometrical structures and various chemical compositions.[17,18] Thus, an adsorption phenomenon is highly connected with the characteristics between the adsorbent and the adsorbed molecules. As described in the previous section, the results of isosteric enthalpy of adsorption, exhibited the existence of surface energetic heterogeneity for the two samples. To get information on surface heterogeneity of an adsorbent, one can use a distribution function, a local adsorption isotherm, and an experimental adsorption equilibrium data. The overall adsorption isotherm on the heterogeneous solid surface can be written in the form of:

$$\theta(p) = \int_{E_{min}}^{E_{max}} \theta(p,E)\, F(E)\, dE \quad T = \text{constant} \quad (7)$$

where p is the equilibrium pressure, E is the adsorption energy, $F(E)$ is the adsorption energy distribution function, ■(p,E) is a local adsorption isotherm with an adsorption energy, and ■(p) is the experimental adsorption isotherm data. This Fredholm integral equation is the first of its kind. The calculation of this distribution function is the well-known ill-posed problem.[19] The two main difficulties in solving the equation are (i) small variations in the experimental data may lead to large changes in the distribution function and (ii) a large set of possible solutions to this equation can produce a distorted result. In general, a proper solution of the integral equation can be obtained from the analytical methods, numerical methods, and local adsorption isotherm approximation methods. In the current work, the generalized nonlinear regularization method was adopted to solve the integral equation, since it can avoid the difficulties caused by the ill-posed nature of an adsorption integral equation.[20] The Fowler Guggenheim isotherm equation was used as a kernel function for this system to describe the localized monolayer adsorption with lateral interaction.

The Fowler Guggenheim (FG) equation is expressed as follows:

$$\theta(p,E) = \frac{Kp\ \exp\left(\frac{zw\theta}{k_BT}\right)}{1 + Kp\ \exp\left(\frac{zw\theta}{k_BT}\right)} \quad (8)$$

where T is the absolute temperature, p is the equilibrium pressure, z is the number of closest adjacent molecules in the monolayer, w is the interaction energy between the two nearest neighboring molecules, k_B is the Boltzmann constant, $K = K_0(T)\ \exp(E/k_BT)$ is the Langmuir constant, and the preexponential factor $K_0(T)$ can be calculated from the partition functions for an isolated molecule.

To examine the adsorption energy distributions, the BET method was used to obtain the monolayer coverage that corresponds to the maximum relative pressure. The determined adsorption energy distributions, $F(E)$, for nitrogen and benzene on the A–10 and PAN carbon nanofibers are shown in Figure 5. For all calculations, the z, zw/k_B, and regularization parameter were assumed to be 4, 380 K and 1×10^{-3}, respectively. The adsorption energy distribution curves of nitrogen obtained for two samples mainly exhibited three peaks. For example, in the case of A–10, the lowest and highest energy peaks appeared at 5.4 and 13.1 kJ mol^{-1} while PAN carbon nanofibers showed the curves at 5.2 and 9.3 kJ mol^{-1} respectively. In addition to these peaks, minor shoulder peaks for two samples were found at about 7.2 (A–10) and 12.5 (PAN carbon nanofibers) kJ mol^{-1}, respectively. Therefore, it is reasonable to suppose from these results that both carbon fibers have the two main energetic states and one tiny state for nitrogen, since the number of peaks is closely related to the surface heterogeneities on the adsorbents. Furthermore, as shown in this figure, similar trends were also observed for the benzene molecule. In other words, the order of the intensity of energy distribution for the two samples revealed the same trends. For example, the calculated energy distribution curves had the highest value for the first peak in A–10 and for the second peak in PAN carbon nanofibers, even though different probe molecules were tested. However, the number of peaks for the adsorption energy distribution of A–10 decreased from three to two. The lower energy distribution curve of benzene for A–10 was in the range of 21–43 kJ mol^{-1} with a maximum at 32.6 kJ mol^{-1}, whereas the higher energy curve was in the range of 44–60 kJ mol^{-1} with a maximum at 52.9 kJ

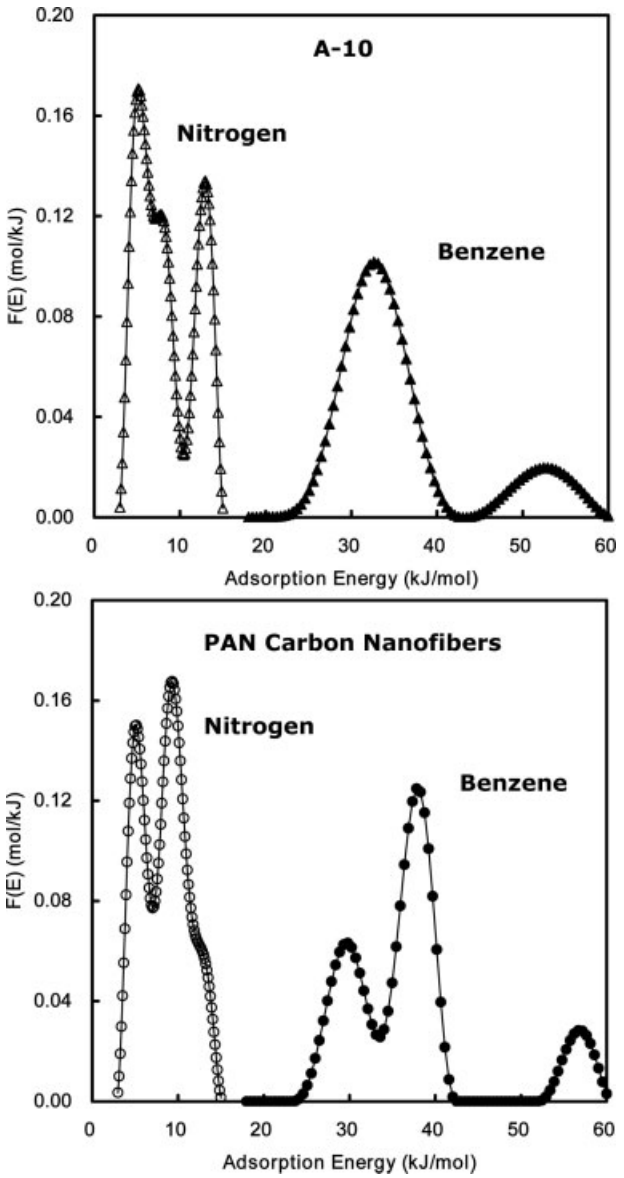

Figure 5 Adsorption energy distribution for nitrogen and benzene on A–10 (top) and PAN carbon nanofibers (bottom) calculated with Fowler–Guggenheim model.

mol^{-1}. The intensity of the first peak for A–10 was about five times higher than that of the second curve. In the case of PAN carbon nanofibers, however, the second peak was around 4.4 times larger than the third and the pronounced peak appeared at about 27.4, 36.4, and 56.7 kJ mol^{-1}, respectively. On the whole, the obtained distribution curves in the present study were in similar ranges obtained for the isosteric enthalpy of adsorption. Moreover, the shapes of the energy distribution curves for benzene on the two carbon fibers were much broader than that of the results for nitrogen molecules, while the A–10 distribution curves were a little bit wider than the curves for PAN carbon nanofibers. These results indicated that PAN carbon nanofibers were more homogeneous than A–10. In addition, the adsorption energy patterns for A–10 were highly associated with probing molecules, while PAN carbon nanofibers had the same energy characteristics, even though the adsorption energy curve of benzene was more pronounced than that of nitrogen. Therefore, these results support a conclusion that both carbon fibers have heterogeneous surfaces, shapes, and trends while the ratios of the peaks are mainly dependent on the structural difference.

Kinetic study

Reliable information on the adsorption kinetics and desorption method is as important as the adsorption equilibria to properly design, simulate, and optimize an adsorber for the removal and recovery of VOCs. In general, assessing the performance of porous adsorbents requires reliable kinetic and desorption information. Since the transport of adsorbates within the porous media is quite complex and the external film mass transfer of adsorbent is relatively fast, it is often applied by assuming that pore diffusion or surface diffusion controlled the intraparticle transport when adsorption occurs at a finite rate.[11,14] Presently, the well-known homogeneous surface diffusion model (HSDM) is based on the existence of an external film at the outer surface of the media and subsequent diffusion in a porous system by Fick's law. The HSDM was selected to describe the adsorption of benzene vapor onto two carbon fibers since the highly favorable isotherms are obtained from adsorption equilibrium data. The mass balance inside a porous particle can be described by the following equation:

$$\frac{\partial q}{\partial t} = D_s \frac{1}{r^s} \frac{\partial}{\partial r} \left(r^s \frac{\partial q}{\partial r} \right) \tag{9}$$

with the initial and boundary conditions as:

$$q(r, t = 0) = 0 \tag{10}$$

$$\left. \frac{\partial q}{\partial r} \right|_{r=0} = 0 \tag{11}$$

$$D_s \left. \frac{\partial q}{\partial r} \right|_{r=R} = k_b (q^* - q) \tag{12}$$

where D_s is the surface diffusivity of adsorbed species along the particle coordinate, s is the particle shape factor, k_b is the barrier resistance, q is the sorbate concentration in the particle, q^* is the surface concentration in equilibrium in the gas phase, r is the radial coordinate, and R is the radius of the adsorbent. To solve this equation, the orthogonal collocation method (OCM) was applied. The detailed description of the solving method was presented

elsewhere.[21] To find the optimum kinetic parameters (D_s and k_b), the Nelder–Mead simplex method was used, because it is based on a comparison of the difference between the experimental and predicted adsorbed amount uptake curves.[15]

The typical adsorption uptake curves for benzene with a temperature of 343.15 K for A–10 and PAN carbon nanofibers are shown in Figure 6 (top). In this study, the experimental kinetic data was collected at $P = 0.0$–1.60 kPa (A–10) and $P = 0.0$–1.55 kPa (PAN carbon nanofibers), respectively. The HSDM model described the adsorption uptake curves satisfactorily. This illustrates the faster adsorption uptake for PAN carbon nanofibers compared with the A–10, although its dosing concentration is slightly higher than that of PAN carbon nanofibers. The kinetic parameters determined from the model for A–10 were $k_b = 2.488 \times 10^{-2}$ s^{-1} and $D_s = 7.607 \times 10^{-11}$ m^2 s^{-1} while those for PAN carbon nanofibers were $k_b = 2.075 \times 10^{-2}$ s^{-1} and $D_s = 1.204 \times 10^{-10}$ m^2 s^{-1}. The results show that the surface diffusivity obtained for PAN carbon nanofibers is one-order-of magnitude greater than that of A–10, although the external film resistances are in the same region.

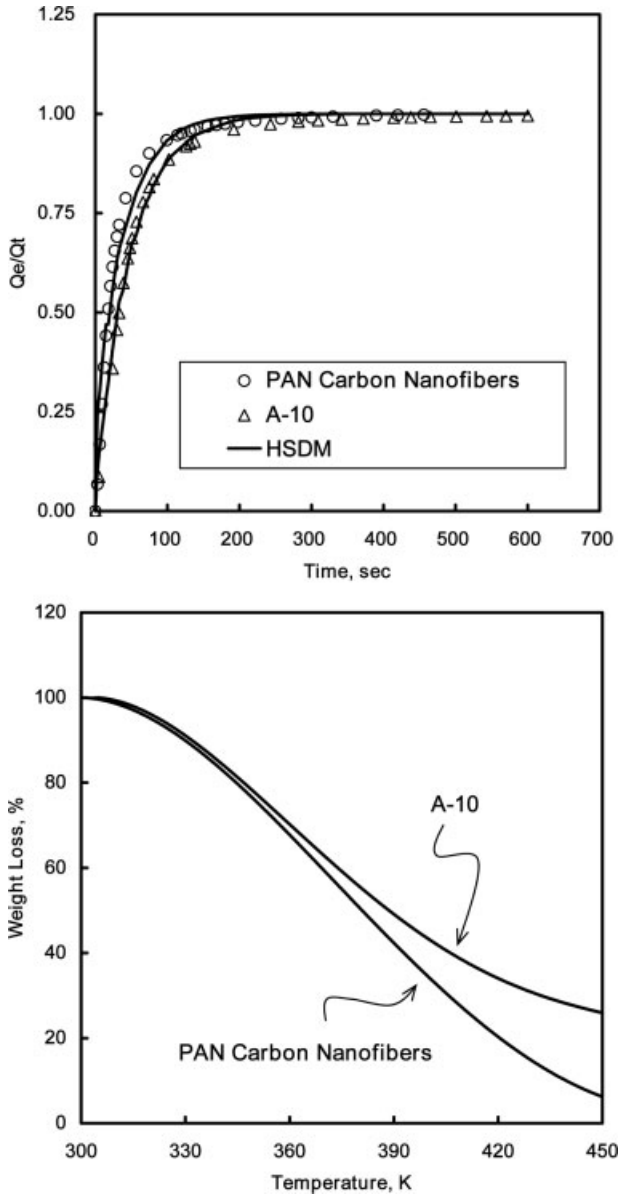

Figure 6 Adsorption kinetic curves at 343.15 K (top) and thermal desorption curves (bottom) of benzene on A–10 and PAN carbon nanofibers at a heating rate of 2 K min^{-1} (Partial pressure = 1.55 kPa).

To examine the characteristics of desorption, the thermal gravimetric (TG) desorption method was used because it is known to be helpful in understanding physical adsorption, pore configuration, organophilicity, and the relationship between the adsorbates.[22] After adsorbing the benzene vapor under isothermal condition (300.15 K), the system was heated at a heating rate of 2 K min^{-1} to desorb the attached adsorbates on sample fibers. Figure 6 (bottom) shows the comparison of the weight loss profiles of benzene on PAN carbon nanofibers and A–10. As shown in this figure, PAN carbon nanofibers have a higher desorbing rate than A–10. The difference gradient of weight loss was negligible at the initial stage; however, as the temperature increased the difference between the two samples diverged markedly. In addition, we observed that the decreased weight ratio of benzene for A–10 and PAN carbon nanofibers was about 75 and 94% at 450.15 K. The major difference seems to be related mainly with their different fiber structure and sizes (D_p) (A–10 = 18 μm and PAN carbon nanofibers = 0.4 μm) since the physical properties of these fibers such as specific surface area, pore volume, and average pore sizes are within the same ranges.

CONCLUSIONS

To assess the feasibility of PAN carbon nanofibers prepared through the electrospinning method for removing and recovering the solvent vapors from industrial effluents, the adsorption properties were examined in terms of nitrogen and benzene adsorption equilibrium, adsorption energy distribution, as well as kinetic and thermal desorption. PAN carbon nanofibers were found to be microporous materials with small amounts of mesopore regions and also with higher adsorption capacities for benzene than for commercial ACFs. The adsorption equilibrium data measured at three different temperatures (343.15, 383.15, and 423.15) K with pressure up to 4 kPa fitted well with the Toth equation, which was also used to interpret the adsorption affinity and isosteric enthalpy of adsorption. The orders of magnitude for Henry's constant and isosteric enthalpy of adsorption were reversed at 383.15 K and 1.5 mol kg^{-1}, respectively. The results of isosteric enthalpy of adsorption and adsorption energy distribution gave important clues for surface features and adsorbate–

adsorbate interaction. These indicated that PAN carbon nanofibers have energetically and structurally heterogeneous surfaces. However, PAN carbon nanofibers surfaces seem to be more homogeneous than A–10 surfaces.

The homogeneous surface diffusion mechanism was used to assess the performance of activated carbon fibers and to determine their kinetic values by comparing the difference between the experimental and predicted adsorbed amount uptake curves obtained from gravimetric adsorption apparatus. The kinetic value of PAN carbon nanofibers obtained clearly exhibited a shallow pore structure, and faster than A–10. Furthermore, compared with the performance of the thermal desorption of A–10, PAN carbon nanofibers has only about a 6% irreversible adsorption amount. Considering the characteristics of adsorption, desorption, and kinetic energy, it can be concluded that PAN carbon nanofibers have the potential for taking part in the removal of VOCs.

The authors thank MCIE, Korea, for financially supporting this research ''Next Generation Growth Engine,'' of Ministry of Science and Technology.

References

1. Ruddy, E. N.; Carroll, L. A. Chem Eng Prog 1993, 89, 28.
2. Khan, I.; Ghoshal, A. K. J Loss Prev Process Ind 2000, 13, 527.
3. Takeshi, Y.; Shigeta, A. Sep Sci Technol 1993, 3, 46.
4. Katsumi, K. J Membr Sci 1994, 96, 59.
5. Kim, C.; Yang, K. S. Appl Phys Lett 2003, 83, 1216.
6. McCann, J. T.; Li, D.; Xia, Y. J Mater Chem 2005, 15, 735.
7. Kim, C. J Power Sources 2005, 142, 382.
8. Chun, I. S.; Reneker, D. H.; Fong, H.; Fang, X. Y.; Deitzel, J.; Tan, N. B.; Kearns, K. J Adv Mater 1999, 31, 36.
9. Reneker, D. H.; Chun, I. S. Nanotechnology 1996, 7, 216.
10. Shim, W. G.; Lee, J. W.; Moon, H. J Chem Eng Data 2003, 48, 286.
11. Lee, J. W.; Shim, W. G.; Moon, H. Microporous Mesoporous Mater 2004, 73, 109.
12. Li, Z.; Kruk, M.; Jaroniec, M.; Ryu, S. K. J Colloid Interface Sci 1998, 204, 151.
13. Valenzuela, D. P.; Myers, A. L. Adsorption Equilibrium Data Handbook; Prentice Hall: Englewood Cliffs, NJ, 1989.
14. Do, D. D. Adsorption Analysis: Equilibrium and Kinetics; Imperial College Press: London, 1998.
15. Riggs, J. B. An Introduction to Numerical Methods for Chemical Engineers; Texas Technological University Press: Lubbock, TX, 1988.
16. Hill, T. L. J Chem Phys 1949, 17, 520.
17. Jaroniec, M.; Madey, R. Physical Adsorption on Heterogeneous Solids; Elsevier: Amsterdam, 1988.
18. Rudzinski, W.; Everett, D. Adsorption of Gases on Heterogeneous Solid Surfaces; Academic Press: London, 1991.
19. Szombathely, M. V.; Brauer, P.; Jaroniec, M. J Comput Chem 1992, 13, 17.
20. Roth, T.; Marth, M.; Weese, J.; Honerkamp. J Comput Phys Commun 2001, 139, 279.
21. Villadsen, J.; Michelsen, M. L. Solution of Differential Equation Models by Polynomial Approximation; Prentice-Hall: Englewood Cliffs, 1978.
22. Zhao, X. S.; Lu, G. Q.; Hu, X. Colloids Surf A 2001, 179, 261.